

## REPORT DOCUMENTATION PAGE

Form Approved OMB NO. 0704-0188

Public Reporting Burden for this collection of information is estimated to average 1 hour per response, including the time for reviewing instructions, searching existing data sources, gathering and maintaining the data needed, and completing and reviewing the collection of information. Send comment regarding this burden estimate or any other aspect of this collection of information, including suggestions for reducing this burden, to Washington Headquarters Services, Directorate for Information Operations and Reports, 1215 Jefferson Davis Highway, Suite 1204, Arlington VA, 22202-4302, and to the Office of Management and Budget, Paperwork Reduction Project (0704-0188), Washington DC 20503

1. AGENCY USE ONLY (Leave Blank)	2. REPORT DATE: 24-Jul-2007	3. REPORT TYPE AND DATES COVERED Final Report      1-Aug-2006 - 30-Apr-2007	
4. TITLE AND SUBTITLE A Novel MEMS Platform for Mechanical Testing of Polymeric Nanofibers		5. FUNDING NUMBERS W911NF-06-1-0356	
6. AUTHORS Ioannis Chasiotis, Nancy Sottos		8. PERFORMING ORGANIZATION REPORT NUMBER	
7. PERFORMING ORGANIZATION NAMES AND ADDRESSES University of Illinois - Urbana Grants and Contracts Office 109 Coble Hall Champaign, IL			
9. SPONSORING/MONITORING AGENCY NAME(S) AND ADDRESS(ES) U.S. Army Research Office P.O. Box 12211 Research Triangle Park, NC 27709-2211		10. SPONSORING / MONITORING AGENCY REPORT NUMBER 51031-EG-II.1	
11. SUPPLEMENTARY NOTES The views, opinions and/or findings contained in this report are those of the author(s) and should not be construed as an official Department of the Army position, policy or decision, unless so designated by other documentation.			
12. DISTRIBUTION AVAILABILITY STATEMENT Distribution authorized to U.S. Government Agencies Only, Contains Proprietary		12b. DISTRIBUTION CODE	
13. ABSTRACT (Maximum 200 words) The abstract is below since many authors do not follow the 200 word limit			
14. SUBJECT TERMS MEMS, NANOFIBERS, MECHANICAL BEHAVIOR		15. NUMBER OF PAGES Unknown due to possible attachments	
		16. PRICE CODE	
17. SECURITY CLASSIFICATION OF REPORT UNCLASSIFIED	18. SECURITY CLASSIFICATION ON THIS PAGE UNCLASSIFIED	19. SECURITY CLASSIFICATION OF ABSTRACT UNCLASSIFIED	20. LIMITATION OF ABSTRACT UL

## Report Title

A Novel MEMS Platform for Mechanical Testing of Polymeric Nanofibers

### **ABSTRACT**

The objective of this project is the design and fabrication of a platform to study the mechanical behavior of electrospun polymer nanofibers. Among different methods of mechanical characterization of nanofibers such as nanoindentation, bending tests, and tensile testing, the latter is considered here as the primary approach to study the mechanical behavior of polymer nanofibers because of its advantages over other methods in investigating different mechanical behaviors including strain rate dependent mechanical responses and large deformations, both of which are expected in polymer nanofibers. Due to high ductility of electrospun nanofibers, the test platform should be capable of generating deformations of 100  $\mu\text{m}$  on 25  $\mu\text{m}$  long sample, while the net axial force applied on the fibers can be as high as 100  $\text{N}$ . The tensile testing apparatus described here for the above purposes is a MEMS device actuated using an on-chip MEMS capacitive based actuator, called nanotractor, with grips to mount the sample, in which the axial force in the sample is measured by a leaf spring MEMS loadcell. Using on-chip actuator eliminates sample misalignment and off-axis loading that could occur in case of external actuation.

---

### **List of papers submitted or published that acknowledge ARO support during this reporting period. List the papers, including journal references, in the following categories:**

#### **(a) Papers published in peer-reviewed journals (N/A for none)**

**Number of Papers published in peer-reviewed journals:**

---

#### **(b) Papers published in non-peer-reviewed journals or in conference proceedings (N/A for none)**

**Number of Papers published in non peer-reviewed journals:**

---

#### **(c) Presentations**

(1) 05-04-2007: Invited Presentation: Center for Nanoscale Science and Technology Annual Conference, University of Illinois at Urbana-Champaign, IL

(2) 05-07-2007: ASME Applied Mechanics and Materials Conference, June 3-7, 2007, University of Texas at Austin, Austin TX.

**Number of Presentations:** 2.00

---

#### **Non Peer-Reviewed Conference Proceeding publications (other than abstracts):**

**Number of Non Peer-Reviewed Conference Proceeding publications (other than abstracts):** 0

---

#### **Peer-Reviewed Conference Proceeding publications (other than abstracts):**

**Number of Peer-Reviewed Conference Proceeding publications (other than abstracts):** 0

---

#### **(d) Manuscripts**

M. Naraghi, I. Chasiotis, Y. Dzenis, Y. Wen, "Strain rate dependent mechanical deformation and failure modes of electrospun polyacrylonitrile nanofibers", in revision in Applied Physics Letters, (2007).

**Number of Manuscripts:** 1.00

---

**Number of Inventions:****Graduate Students**

<u>NAME</u>	<u>PERCENT SUPPORTED</u>
Thomas Berfield	0.50
<b>FTE Equivalent:</b>	<b>0.50</b>
<b>Total Number:</b>	<b>1</b>

**Names of Post Doctorates**

<u>NAME</u>	<u>PERCENT SUPPORTED</u>
<b>FTE Equivalent:</b>	
<b>Total Number:</b>	

**Names of Faculty Supported**

<u>NAME</u>	<u>PERCENT SUPPORTED</u>	National Academy Member
Ioannis Chasiotis	0.00	No
Nancy Sottos	0.00	No
<b>FTE Equivalent:</b>	<b>0.00</b>	
<b>Total Number:</b>	<b>2</b>	

**Names of Under Graduate students supported**

<u>NAME</u>	<u>PERCENT SUPPORTED</u>
<b>FTE Equivalent:</b>	
<b>Total Number:</b>	

**Student Metrics**

This section only applies to graduating undergraduates supported by this agreement in this reporting period

The number of undergraduates funded by this agreement who graduated during this period: ..... 0.00

The number of undergraduates funded by this agreement who graduated during this period with a degree in science, mathematics, engineering, or technology fields:..... 0.00

The number of undergraduates funded by your agreement who graduated during this period and will continue to pursue a graduate or Ph.D. degree in science, mathematics, engineering, or technology fields:..... 0.00

Number of graduating undergraduates who achieved a 3.5 GPA to 4.0 (4.0 max scale):..... 0.00

Number of graduating undergraduates funded by a DoD funded Center of Excellence grant for Education, Research and Engineering:..... 0.00

The number of undergraduates funded by your agreement who graduated during this period and intend to work for the Department of Defense ..... 0.00

The number of undergraduates funded by your agreement who graduated during this period and will receive scholarships or fellowships for further studies in science, mathematics, engineering or technology fields: ..... 0.00

**Names of Personnel receiving masters degrees**

<u>NAME</u>
-------------

<b>Total Number:</b>
----------------------

---

**Names of personnel receiving PhDs**

NAME

**Total Number:**

**Names of other research staff**

NAME

PERCENT SUPPORTED

**FTE Equivalent:**

**Total Number:**

**Sub Contractors (DD882)**

**Inventions (DD882)**

## **Final Project Report - Grant # W911NF-06-1-0356**

**Reporting Period: August 2006 – April 2007**

### **A Novel MEMS Platform for Mechanical Testing of Polymeric Nanofibers**

PI: Ioannis Chasiotis, co-PI: Nancy Sottos

Beckman Institute for Advanced Science and Technology

University of Illinois at Urbana-Champaign, Urbana IL 61801

#### **I. Statement of the Problem Studied**

The objective of this project was the design and fabrication of a MEMS platform to study the mechanical behavior of electrospun polymer nanofibers. Among different methods of mechanical characterization of nanofibers such as nanoindentation, bending tests, and tensile testing, the latter was considered as the primary approach to study the mechanical behavior of polymer nanofibers because of its advantages over other methods in investigating different mechanical behaviors, including strain rate dependent mechanical response and large deformations, both of which are expected in polymer nanofibers. Due to the high ductility of electrospun nanofibers, such a microscale testing platform must be capable of generating deformations of 100  $\mu\text{m}$  on 25- $\mu\text{m}$  long sample, while the net axial force applied on the fibers must be as high as 100  $\mu\text{N}$ . The tensile testing apparatus developed under this STIR program is a MEMS device actuated using an on-chip MEMS capacitive based actuator, nanotractor, with grips to mount the sample, in which the axial force in the sample is measured by a leaf spring MEMS loadcell. Using on-chip actuator eliminated sample misalignment and off-axis loading.

For small diameter samples (10-100 nm range), many issues arise when attempting to image and grasp an individual fiber for testing. The width of these fibers is well below the Raleigh limit and the resolving power of standard optical microscopes. Often times a scanning electron microscope (SEM) is used to image fibers in the nanoscale regime. However, with PAN fibers the environment necessary for SEM imaging significantly alters the material properties. Our solution was to label the nanoscale PAN fibers with a fluorescent dye. Under the proper excitation, the fibers fluoresce to a size scale that is visible using standard optical microscopy. Optical imaging of the fibers enabled manipulation and testing similar to that performed with larger fibers. The determination of a method for attaching a fluorescent dye to the PAN fibers was the subject of this project.

## II. Methods and Procedures

The MEMS tensile testing platform was designed for mechanical characterization of polymer nanofibers in a wide range of mechanical behaviors including large deformations and strain rate dependent mechanical behaviors. This device has just (7/24/2007) been fabricated by the Sandia National Laboratory through Sandia ultra-planar, multi level technology of MEMS fabrication (SUMMiT V<sup>TM</sup>) process. The fabrication process took approximately three months.

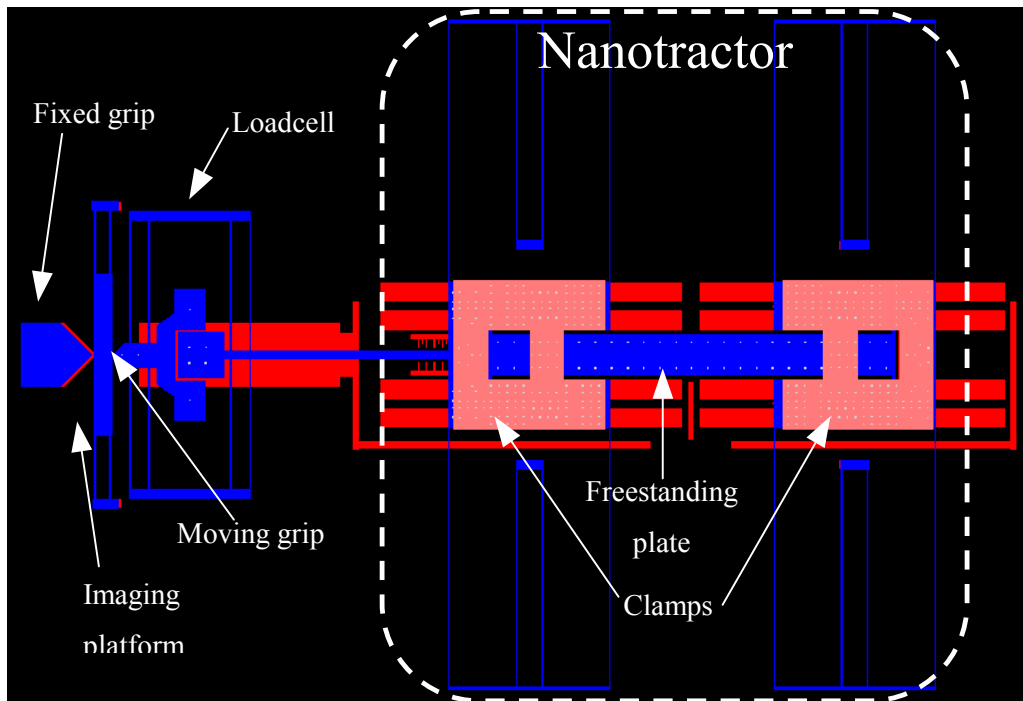


**Figure 1.** Schematic of the MEMS tensile testing device. The main parts are: Fixed and moving grips to mount the fiber, imaging platform, load cell, and the actuator.

The MEMS tensile testing platform consists of the following parts, Figure 1:

- Fixed and moving grips, on which the fiber is mounted with its two ends adhered to the pads for the tension test using an appropriate adhesives. The distance between the grips in the as fabricated device is 25  $\mu\text{m}$ , which is the gage length of the polymer nanofiber samples. This gage length was chosen based on our previous experiments on polymer fibers. One of the grips is anchored to the substrate, and the other is attached to the loadcell. The gage length can be increased or decreased by actuating the nanotractor before mounting the sample.
- Imaging platform, is a freestanding plate incorporated in the gage section of the tension test platform, on which the sample rests during sample mounting and during post processing after the

tension test under SEM. Before the tension test, the sample is mounted on the MEMS device, with its gage section laying on the imaging platform. During testing, the platform is bent down capacitively, by applying a voltage between the plate and the substrate.

- Load cell, which is a pair of folded beams. This load cell consists of two identical folded beams acting in parallel, each with the theoretical stiffness of 1.5 N/m. Using Focused ion beam, any of the pairs of folded beams can be cut to obtain higher force resolution. The relative motion of the two ends of the load cell will be measured to calculate the tensile force on the fibers.
- Actuator, which is a nanotractor designed and fabricated by the Sandia National Lab primarily to study the friction and wear in MEMS devices [1]. This actuator is a capacitive based surface micromachined actuator with the travel range of 60-80  $\mu\text{m}$ , which is capable of generating forces of a few hundreds of micronewtons on the sample with little or no temperature changes. It allows for different actuation velocities, which results in a wide range of strain rates. The device consists of a freestanding plate that is connected to two clamps on its two opposite sides. The clamps are free standing over the substrate through some tethers. By appropriate sequencing of the bias voltages between each of the three parts and the substrate, the actuator starts to move. The design of this actuator was kindly provided by Dr. de Boer from Sandia National labs for the purpose of implementing in this design.

Mechanical design of the components of the device such as the loadcell and the imaging platform were performed in UIUC based on the mechanical properties of the structural layers provided by Sandia National labs, and the layout for the fabrication was generated in a CAD software environment (AutoCAD 2007) enhanced with *2D-3D visualization* and *MEMS design* tools provided by Sandia. The design was submitted to Sandia National labs for fabrication in early April of 2007, and the first tests will be conducted by early September. The whole tension tests will be performed and recorded under an optical microscope, and the deformations of the loadcell and the fiber will be measured using the digital image correlation (DIC) algorithm by comparing the images of the deformed configuration of the device with the images from the initial configuration as explained in [2].

The successive steps of the tension test on a single nanofiber are shown in Figure 2. To perform the test, the fiber sample will be mounted on the device with its two ends adhered to the grips (Figure 1) using high viscosity adhesives. The procedure for sample manipulation is explained in [2,3]. To start the tension test, first, imaging platform is actuated to release the fiber. Then, by actuating the nanotractor (motion to the right in Figure 2) the fiber is stretched. The imaging platform is used several times during the test to AFM image the deformed fiber. This procedure continues until the fiber fails, and the broken halves of the fiber will be observed with SEM for further studies. It is to be noted that due to the

vulnerability of the polymer nanofibers to ebeam inside the SEM chamber, any type of SEM imaging before the tension test should be prohibited.

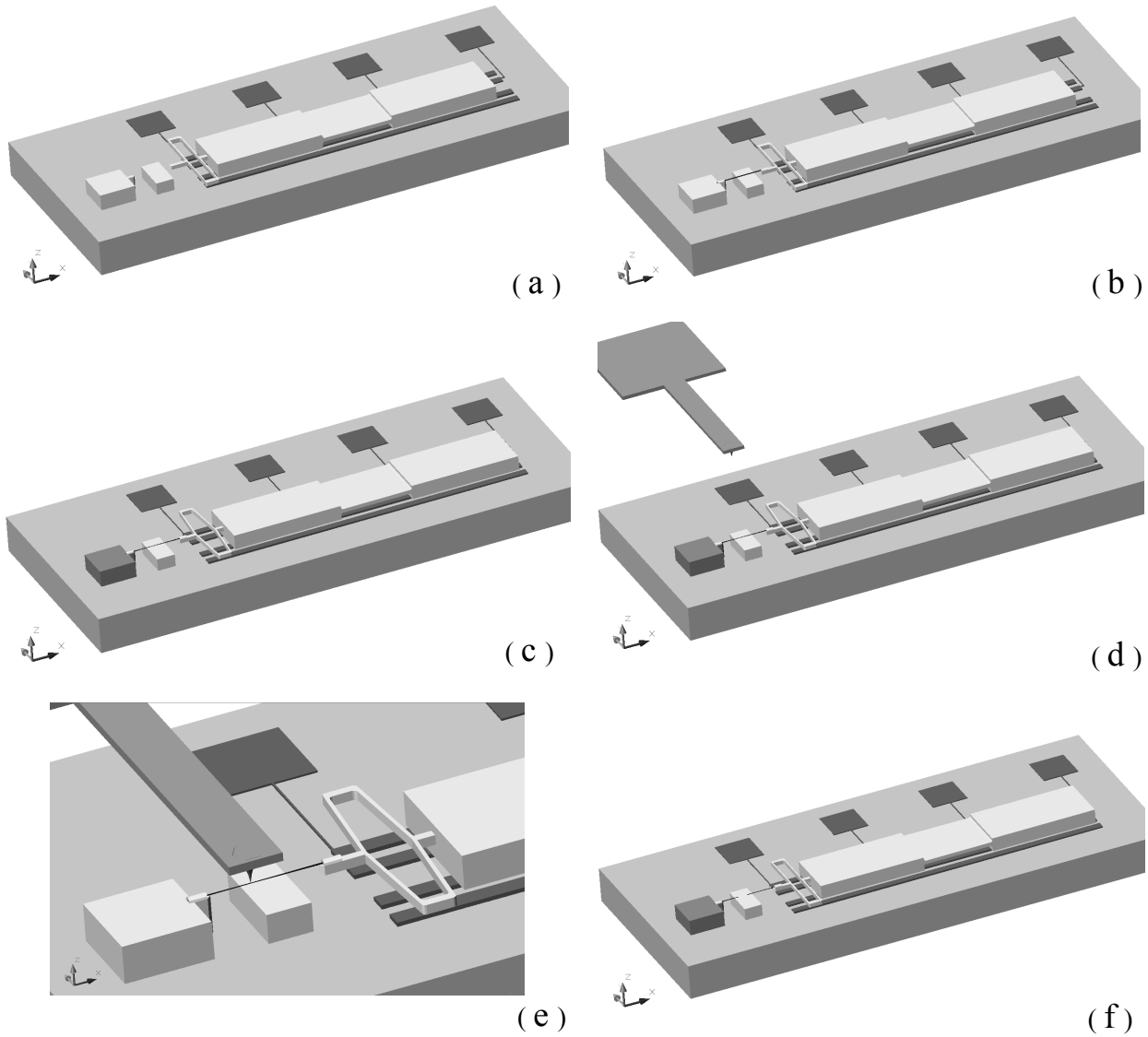


**Figure 2.** Successive steps of the tension test on electrospun polymer nanofibers. **(a)** Device before sample preparation, **(b)** fiber sample manipulated and mounted on the device, **(c)** fiber after the nanotractor is being actuated, **(d)** AFM cantilever brought close to the fiber to image the fiber, **(e)** AFM tip imaging the deformed fiber **(f)** broken fiber.

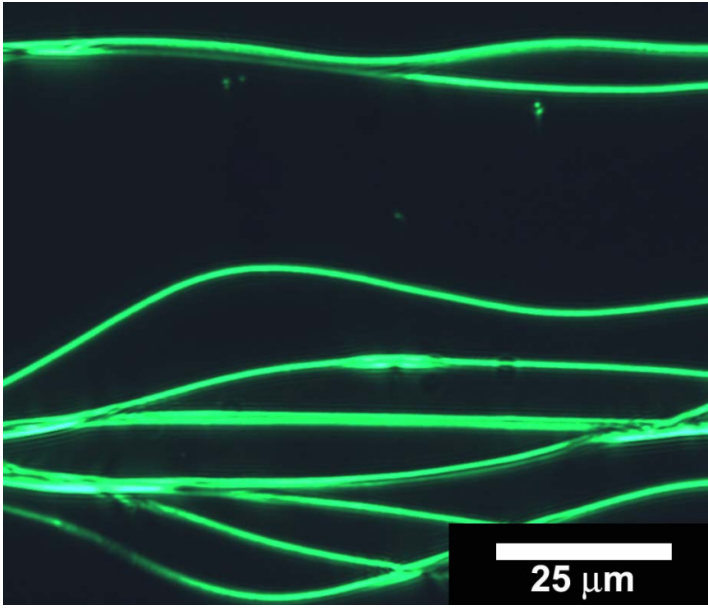


**Figure 3.** Polyacrylonitrile (PAN) fibers coated with a fluorescein based dye under fluorescent excitation.

were dried under a stream of filtered nitrogen. An alternative option, not attempted, would be to incorporate a dye into the precursor polyacrylonitrile solution prior to electrospinning fibers. Similar to whitening agent additives, this may lead to enhanced imaging properties. Mechanical properties and fiber dimensions, though, may be affected depending on the dye concentration.

On the other front, to test the feasibility of the labeling PAN fibers with a fluorescent dye, larger diameter PAN fibers (600 nm to 1.5  $\mu$ m). The least intrusive method of attaching the dye was attempted which involved dipping the fibers in a bath containing a concentrated fluorophore in a solution of ethanol. For this technique, two different fluorescent dyes were used: a commercial fluorescein based dye (max. excitation wavelength of 494nm) and rhodamine B isothiocyanate (max. excitation wavelength of 555nm). The PAN fibers were kept immersed in the dye bath for 1 hour, after which they

### III. Summary of Important Results

The device described above will be used this Fall to investigate the mechanical behavior of electrospun polymer nanofibers with diameters in the range of 100nm - 1 $\mu$ m, ultimate strains of a few hundred percents and strength of less than 100 MPa. The resolution of the device in measuring strains and stresses depends on the fiber diameter and the initial fiber length. Thicker fibers will provide better resolution in measuring the stresses in the fiber because of the limited resolution in force measurement, and better strain resolution is achieved for longer samples because of the displacement resolution. Part of this project's effort has been included in a recently submitted article in Applied Physics Letters that is currently under review and it is attached to this document [3].

*This MEMS design has been submitted to the Sandia MEMS Design Competition, and Prof. Chasiotis (PI) and his graduate student received the First Prize in Sandia MEMS Design Competition on “Novel MEMS Devices for Nanoscale Phenomena” see web:*

*(<http://www.sandia.gov/news/resources/releases/2007/university-mems.html>)*

In terms of nanofiber staining, for both solutions used, the PAN fibers allowed an adequate amount of dye to absorb onto the surface to be fluorescently imaged. Figure 3 shows fibers immediately after coating with the fluorescein dye. The PAN fibers coated with the rhodamine dye are shown in Figure 4a under normal imaging conditions (white light, no frequency cut-off filters), and the same fibers under fluorescent excitation. Either is a viable option for imaging nanoscale PAN fibers during the manipulation stage of mechanical testing. Figure 5 shows a higher magnification image of a rhodamine coated PAN fiber, which is similar to the imaging conditions that would be necessary for nanoscale fibers. The major concern with this method is that over an extended time of excitation, fluorescent dyes generally photobleach, or lose their emitted light intensity. By contrast, the rhodamine coated fibers remained easily imaged after extended fluorescent excitation. The samples lost little intensity after 10 minutes of constant, high intensity excitation. This timeframe should be sufficient to allow for the fibers to be imaged, acquired, and placed in the testing apparatus.

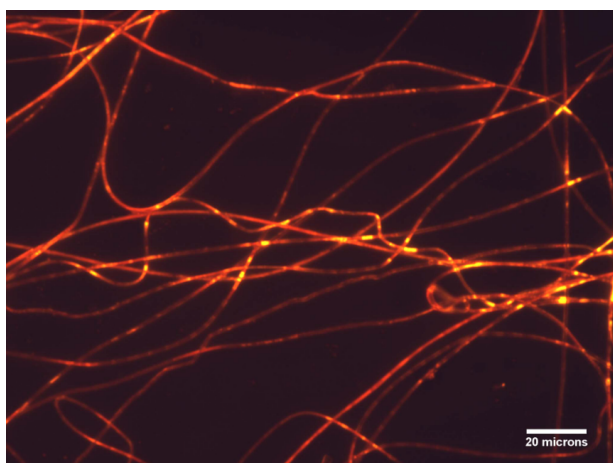


**Figure 4.** PAN fibers coated with a rhodamine based dye under **(a)** normal and **(b)** fluorescent excitation imaging conditions

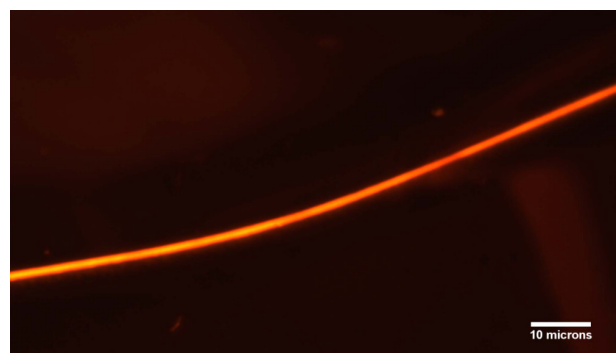


**Figure 5.** High magnification optical microscope image of a single 1.3  $\mu\text{m}$  diameter PAN fiber under **(a)** normal and **(b)** fluorescent excitation imaging conditions

#### IV. Bibliography

- [1] De Boer M. P. Luck D. L. Ashurst W. R. Maboudian R. Corwin A. D. Walraven. J. A. Redmond J. M. *J. Microelectromech. Syst.* **13**, pp. 63-74 (2003).
- [2] Naraghi M Chasiotis I Wen Y and Dzenis Y *Proceedings of 2007 SEM conference Springfield MA* (2007).
- [3] Naraghi, M. Chasiotis, I. Dzenis, Wen, Y. "Strain rate dependent mechanical deformation and failure modes of electrospun polyacrylonitrile nanofibers", in revision in *Applied Physics Letters*, (2007).

## Strain rate dependence of mechanical deformation and failure of electrospun polyacrylonitrile nanofibers

Mohammad Naraghi and Ioannis Chasiotis

*University of Illinois at Urbana Champaign, Aerospace Engineering, 325 Talbot Lab, 104 S. Wright Street, Urbana, IL 61801*

Harold Kahn

*Case Western Reserve University, Department of Materials Science and Engineering Cleveland, OH 44106-7204*

Yongkui Wen and Yuris Dzenis

*Department of Engineering Mechanics, University of Nebraska, Lincoln, NE 68588-0526*

The mechanical deformation of 12- $\mu\text{m}$  long electrospun polyacrylonitrile (PAN) nanofibers with diameters 300-600 nm, subjected to cold drawing rates between  $10^{-2}$  -  $10^{-4} \text{ s}^{-1}$  were investigated by using a surface micromachined mechanical testing platform. The ultimate strain of the PAN nanofibers tested in air was 60-120% varying monotonically with the strain rate. On the contrary, the fiber tensile strength, ranging between 40-130 MPa, varied non-monotonically with the slowest drawing rate resulting in the largest ductilities and fiber strengths. This anomalous behavior was due to distinctly different structural deformations at different loading rates. At the two faster rates, the large fiber ductility originated in the formation of ripples (necks), while at the slowest strain rate, the nanofibers deformed homogeneously allowing for increased applied force and engineering strengths.

The first report on fine electrospun fibrils prepared from solution dates in 1934<sup>1</sup>. Recently, this method has received considerable attention and electrospun fibers have been introduced as reinforcements in composites to enhance the matrix fracture toughness<sup>2</sup>. Furthermore, due to their biophysical and mechanical compatibility with natural tissues and their biodegradability, electrospun nanofibrous structures have been proven to be effective scaffolds for repair of damaged tissues<sup>3,4,5</sup>.

The mechanical behavior of electrospun polymeric nanofibers is expected to differ from bulk and microscale fibers due to the fabrication process and the large surface-to-volume ratio. Determining their mechanical properties, however, is not a straightforward task, mainly because of their very small dimensions and fragility.

Among different methods for mechanical property testing, tension tests are the most appropriate<sup>6,7,8,9</sup> as polymeric nanofibers can carry only tensile forces. Compared to other methods, such as nanoindentation<sup>10,11</sup>, and bending<sup>12</sup>, tension tests require very few assumptions to extract mechanical properties and they allow for a range of strain rates including creep and stress relaxation.

In the present work, the mechanical behavior of polyacrylonitrile (PAN) electrospun nanofibers was investigated by tensile testing at three nominal strain rates ( $2.5 \cdot 10^{-4}$ ,  $2.5 \cdot 10^{-3}$ ,  $2.5 \cdot 10^{-2} \text{ s}^{-1}$ ). The platform used for these tests was a surface micromachined device with an on-chip leaf-spring loadcell and grips for sample mounting. To allow for large fiber drawing ratios, the test device was translated by a piezoelectric actuator, Fig. 1. Nanofibers were mounted on the grips by a micromanipulator and were attached with a viscous epoxy adhesive. Several tests were conducted to ensure that the adhesive did not wet the fibers. Tension tests were carried out under an optical microscope at 500 $\times$  magnification. The field of view included the grips and the loadcell so that the deflection of the loadcell and the displacements of the fiber grips were extracted synchronously from optical images to compute the applied

force and the fiber elongation. The loadcell deflection and the fiber elongation were computed by the application of digital image correlation (DIC) on the entire device with a resolution in rigid body displacements better than 50 nm<sup>13</sup>.

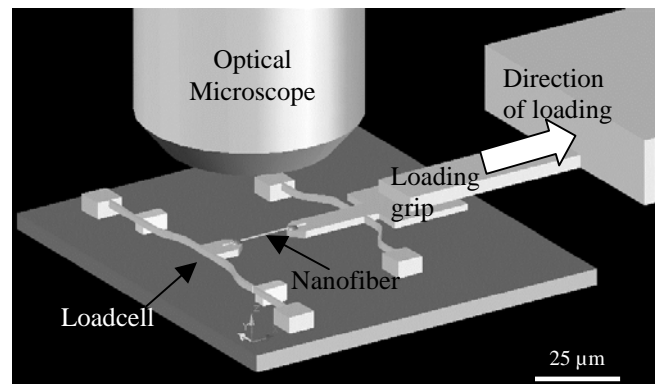


Fig 1. Test platform for nanofiber tension experiments.

The stiffnesses of the loadcells were calculated by a finite element analysis. For the devices used here independent calibration of the loadcells with a pre-calibrated AFM probes were shown to be very close to the finite element estimates. This was owed to the uniform thickness of the device and the precise determination of its dimensions. The undeformed length and diameter of each fiber were measured by optical microscopy and SEM, respectively. The fibers were not exposed to the SEM before testing to avoid embrittlement and loss of ductility, which was found to be as high as 80%. Since the axial force in the fibers and their deformation were measured synchronously, this method for nanoscale mechanical characterization is suitable for tensile tests at varying strain rates.

The basic MEMS platform was fabricated at Case University and it was modified at UIUC by using a Focused Ion Beam (FIB). Fabrication involved the growth of a 2.0-

$\mu\text{m}$  thick silicon dioxide on a (100) silicon wafer and deposition of 2.0- $\mu\text{m}$  silicon dioxide by low pressure chemical vapor deposition (LPCVD) to create a 4.0- $\mu\text{m}$  thick silicon dioxide serving as sacrificial layer. Polysilicon with a thickness of 5.2  $\mu\text{m}$  was deposited by LPCVD and annealed at 1050°C to form the test platform. The polysilicon layer was patterned by photolithography, followed by plasma dry etching. The devices were released in HFA to remove the undesired masking and sacrificial silicon dioxide.

The electrospun nanofibers were fabricated from PAN solution in dimethylformamide, with average molecular weight of 150,000. Electrospinning was conducted at 12.5 kV, with a 20 cm distance from the tip of the stainless steel tube to the bottom plate and at feed rate of 0.2 - 0.5 ml/h. Nanofibers were collected on a TEM grid to facilitate their isolation, handling, and placement onto the test apparatus.

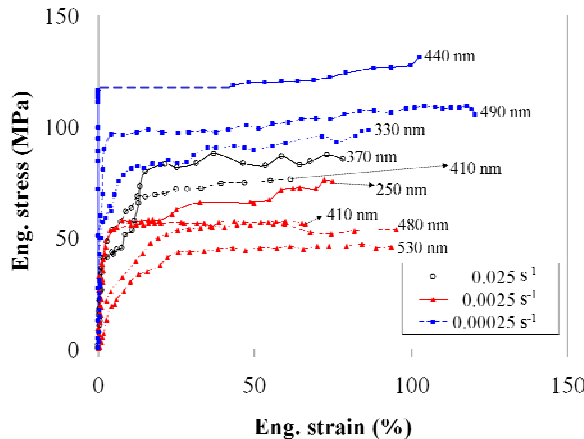


**FIG. 2.** Engineering stress-strain curves of PAN nanofibers at three strain rates. The initial diameters are shown next to each curve (the dashed line at the top curve indicates a lapse in the data acquisition system).

The engineering stress-strain curves of nine PAN electrospun nanofibers obtained in ambient conditions are shown in Fig. 2. All specimens originated in the same target and were subject to the fabrication conditions. The strain rates are the nominal values corresponding to the cross-head motion of the fiber grips representing the loading rate after the onset of plastic deformation when the fibers were drawn at almost constant applied force. In the elastic regime of loading the actual strain rate was smaller than the nominal due to simultaneous extension of the loadcell bars.

The ultimate strain at fiber failure was in the range of 60-120%, monotonically decreasing with strain rate, Fig. 3a. This behavior is generally expected because of the increased relative contribution of creep in material deformation as the strain rate decreases. The fiber strength on the other hand was in the range of 40-130 MPa, and was in good agreement with results reported by Fenessey and Farris for twisted yarns of PAN<sup>14</sup>, i.e. 70-160 MPa. Contrary to the consistent trend in ultimate strain, the tensile strength did not vary monotonically with strain rate,

Fig. 3b. Instead, the highest strength occurred at the slowest strain rate ( $2.5 \cdot 10^{-4} \text{ s}^{-1}$ ), while the smallest strength was recorded at the medium strain rate ( $2.5 \cdot 10^{-3} \text{ s}^{-1}$ ), Fig. 3b. Such behavior is unusual for homogenous material deformations, and thus, the explanation was sought in structural fiber deformations occurring as a result of the competing effects of the external loading rates and the time dependent creep and stress relaxations in the polymeric nanofibers.

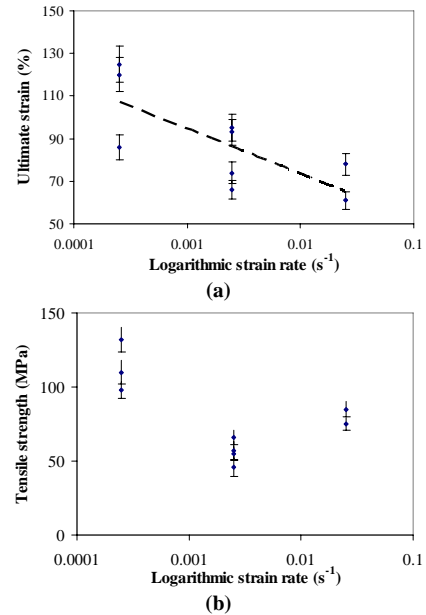


**FIG. 3.** (a) Fiber ultimate strain and (b) tensile strength as a function of strain rate for electrospun PAN nanofibers.

As shown in Fig. 4a, the undeformed nanofibers had uniform cross sections and smooth surfaces. However, at the lowest strain rate, densely-packed fine ripples formed on the fibers during axial deformation, Fig. 4b. The depth of these ripples was 20-40 nm, which were spaced apart by an average distance of 50 nm. The average ultimate engineering strain and the true strain at failure for the samples loaded at the slowest strain rate were 110% and 74%, respectively.

At the faster strain rates the large fiber elongations were due to the formation of a cascade of deep periodic surface ripples (necks), Fig. 4c, that accommodated the displacements induced by the actuator at the fiber ends. As a consequence, the fibers were drawn at smaller applied forces and thus engineering stresses, although the local stress (true stress) in each neck was considerably higher than the engineering stress in Figure 3b. A lower bound of the true stress at the fiber necks at fracture may be obtained by dividing the axial force in the fiber at failure by the neck cross section. Thus, the engineering strength of the fibers shown in figs. 4(b) and 4(c) were 120 MPa and 80 MPa, respectively, while the true strengths were ~180 MPa and 230 MPa (neck section), respectively. In other words, the

fibers that deformed uniformly at the slowest strain rate experienced smaller true stress at failure compared to the fibers drawn at faster strain rates forming deep surface ripples, which is consistent with macroscopic experiments.

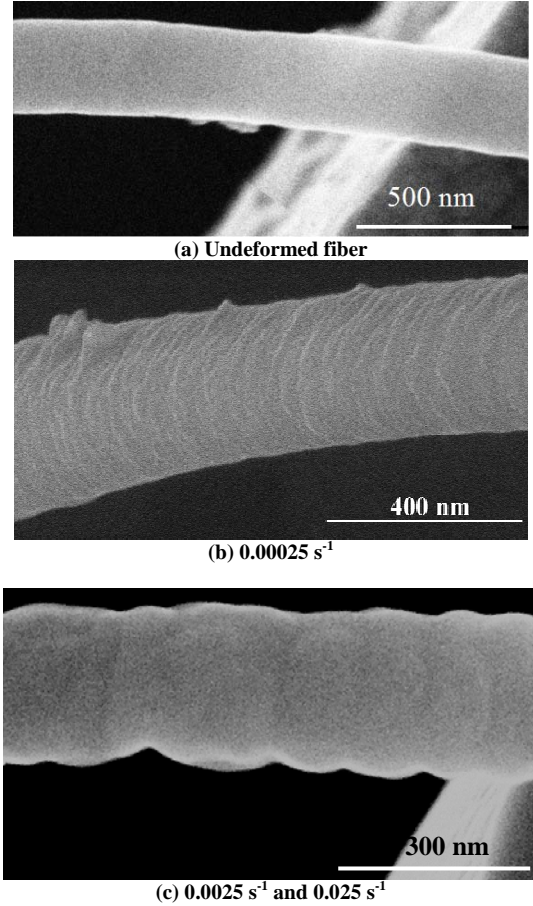


**FIG. 4.** (a) Undefomed PAN nanofiber. (b)-(d) SEM images of the surface morphologies of the deformed fibers at three strain rates.

One reason for the formation of surface ripples, Fig. 4(c), are differences in the time-dependent behaviors of the fiber core and its surface. Different stress relaxation times between the fiber surface and its core resulted in a strain gradient and, thus, shear stresses that initiated the periodic surface ripples, fig. 4(c). The simultaneous formation of surface necks limited their propagation along the fiber length. Thus, neck formation was not accompanied by neck propagation, as it is customary in microscale fibers subject to cold drawing, because adjacent necks mutually limited their propagation. SEM images of fractured fibers, pointed out to the fact that the polymer molecules in the fiber core were subject to conditions encountered in bulk materials as evidenced by the formation of voids in fig. 5(c). On the other hand, surface molecules were subject to reduced lateral constraints because of the free surface.

Contrary to the faster strain rates, at the slowest strain rate, stress relaxation and creep permitted polymer

macromolecules at the fiber surface to rearrange faster than the rate of change in the externally applied stress. Therefore, the nanofibers drawn at  $2.5 \cdot 10^{-4} \text{ s}^{-1}$  deformed uniformly with small variations in their diameter, Fig. 4b. This lack of local structural deformations due to stress localization resulted in increased engineering stress during fiber drawing and larger axial forces in the fiber contrary to the fibers that were subject to faster loading rates.

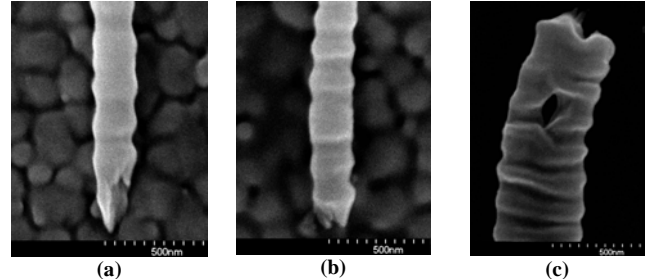


**FIG. 5.** (a-b) Matching surfaces of a fractured PAN nanofiber, and (c) fiber failure due to formation of voids.

Finally, the failure modes of fibers that were subjected to necking are of interest. Contrary to macroscopic neck propagation and failure by reduction in the neck diameter, fracture in several PAN nanofibers was owed to extrusion of a  $45^\circ$  cone from a fiber “bulge”, Fig. 5(a-b). Furthermore, despite the small fiber diameter, fracture due to formation of nanopores in the fiber core, Fig. 5(c), was also observed, which is common in thick polymeric fibers.

The authors acknowledge the support by the National Science Foundation (NSF) under NSF-NIRT grant DMI-0532320, and by the U.S. Army Research Office under grant number W911NF-06-1-0356 with Dr. Bruce LaMattina as the program manager.

- 
- <sup>1</sup> A. Formhals, U.S Patent 1,975,504 (1934).
  - <sup>2</sup> J. S. Kim, and D. H. Reneker, *J. Polym. Compos.* **20**, 124 (1999).
  - <sup>3</sup> W. J. Li, C T Laurencin, E. J. Caterson, R. S. Tuan, and F. K. Ko, *Wiley Periodicals*, 613 (2002).
  - <sup>4</sup> T. Courtney, M. S. Sacks, J. Stankus, J. Guan, and W. R. Wagner, *J. Biomater.* **27**, 3631 (2006).
  - <sup>5</sup> W. J. Li, J. A. Cooper, R. L. Mauck, and R. S. Tuan, *J. Acta Biomater.* **2**, 377 (2006).
  - <sup>6</sup> E. Zussman,M. Burnman, A. L. Yarin, R. Khalfin, and Y. Cohen Y, *J. Polym. Sci., Part B: Polym. Phys.* **44**, 1482 (2006).
  - <sup>7</sup> E. P. S. Tan, and C T. Lim, *J. Rev. Sci. Instrum.* **75**, 2581 (2004).
  - <sup>8</sup> Y. Zhu, and N. Moldovan, *Appl. Phys. Lett.* **86**, 013506 (2005).
  - <sup>9</sup> U. Singh, V. Prakash, A.R. Abramson, W.Chen, L. Qu, L.Dai, *App. Phys. Let.* **89**, 073103 (2006).
  - <sup>10</sup> F. Ko, Y. Gogotsi, A. Ashraf, N. Naguib, H. Ye, G. Yang, C. Li, and P. Willis, *J. Adv. Mater.* **15** 1161 (2003).
  - <sup>11</sup> E. P. S. Tan, and C. T. Lim, *J. Compos. Sci. Technol.* **66**, 1102 (2006).
  - <sup>12</sup> S. Cuenot, S. Demoustier-Champagne, and B. Nysten, *Phys. Rev. Lett.* **85**, 1690 (2000).
  - <sup>13</sup> M. Naraghi, I. Chasiotis, Y. Dzenis, Y. Wen, and H. Kahn, *Rev. Sci. Instrum.*, (2007), Submitted
  - <sup>14</sup> S. F. Fennessey, and R. J. Farris, *Polym. J.* **45**, 4217 (2004).